

Reducing vortex motion in $\text{YBa}_2\text{Cu}_3\text{O}_7$ crystals with splay in columnar defects

L. Civale* and L. Krusin-Elbaum

IBM Research, Yorktown Heights, New York 10598-0218

J. R. Thompson

*Oak Ridge National Laboratory, Oak Ridge, Tennessee 37831-6061
and Department of Physics, University of Tennessee, Knoxville, Tennessee 37996*

R. Wheeler

Argonne National Laboratory, Argonne, Illinois 60439

A. D. Marwick

IBM Research, Yorktown Heights, New York 10598-0218

M. A. Kirk

Argonne National Laboratory, Argonne, Illinois 60439

Y. R. Sun

Department of Physics, University of Tennessee, Knoxville, Tennessee 37996

F. Holtzberg and C. Feild

IBM Research, Yorktown Heights, New York 10598-0218

(Received 8 April 1994)

A strategy to boost the current-carrying capacity of cuprate superconductors beyond the levels attainable with parallel columnar defects was recently proposed. It consists of the enforcement of vortex entanglement by controlled splay of columns. We demonstrate the validity of this suggestion in $\text{YBa}_2\text{Cu}_3\text{O}_7$ single crystals using the difference in splay naturally occurring in irradiations with two ions differing in mass and energy. The terminal dispersion of the columns produced by 0.58-GeV $^{116}\text{Sn}^{30+}$ is about 10° , as compared with 1° for 1.08-GeV $^{197}\text{Au}^{23+}$. At high temperatures, this large splay results in a persistent current density one order of magnitude larger and a creep rate one order of magnitude smaller.

Recently we have shown that aligned columns of damaged material in high-temperature semiconductors, installed by the irradiation with swift (\sim GeV) heavy ions such as Sn, pin magnetic vortices much more effectively than point defects.¹ Generating such disorder is clearly technologically relevant, for it enhances the critical current density J_c by orders of magnitude and considerably expands the useful irreversible regime.¹⁻⁴ Hwa and co-workers⁵ just proposed that a small splay (i.e., a dispersion in the orientation of the columns) will force vortex entanglement, leading to even larger J_c and a smaller vortex creep rate. Here we establish such an effect in $\text{YBa}_2\text{Cu}_3\text{O}_7$ (YBCO) single crystals using the difference in splay naturally occurring in irradiations with two ions differing in mass and in energy, 0.58-GeV $^{116}\text{Sn}^{30+}$ and 1.08-GeV $^{197}\text{Au}^{23+}$. At high temperatures, the larger splay of the tracks produced by Sn irradiation ($\sim 10^\circ$) results in a persistent current density one order of magnitude larger and a creep rate one order of magnitude smaller as compared with Au irradiation with splay $\sim 1^\circ$. We conclude that a considerable further improvement of the current carrying capacity of high-

temperature superconductors can still be obtained.

The trivial reason for the strong and highly directional pinning of magnetic vortices in a type-II superconductor with long columnar defects, comes from the topology of the vortex; it is a linear object which can now be captured over a considerable portion of its length. Strong pinning is, of course, technologically essential, since electrical resistance comes from the dissipation associated with vortex motion. Such a motion is driven by the Lorentz force $\mathbf{F} = \mathbf{J} \times \mathbf{B}$, which acts over the entire length of the vortex, and must be reduced by the pinning force which acts only over the fraction of the vortex length that is pinned. In the case of aligned columnar defects, the fraction can approach unity. This should be contrasted with core pinning by point defects, where only a small fraction of the vortex is pinned.⁶ Moreover, pinning by random point defects involves an extra cost in elastic energy arising from the meandering of the vortex core between pinning centers,⁷ which is absent in the case of columnar defects aligned with the applied magnetic field.

The nontrivial consequence of the aligned disorder is the formation of the thermodynamic state of the vortex

matter: a Bose glass⁸ in which vortices are localized on columnar pins, in analogy to a system of two-dimensional bosons. Thermal fluctuations will allow segments of vortices to “peel off” their tracks,⁸ a process that will be further stimulated at high temperatures by the reduction of the pinning energy due to entropic effects. The reduction of the persistent current due to relaxation will take place via three processes:⁸ (i) the formation of the half-loop excitations, which grow; (ii) the double-kink formation in the vortex line, allowing it to reside on two tracks; and (iii) the spread of the double kinks, which is entirely unimpeded for parallel tracks at high temperatures.⁸

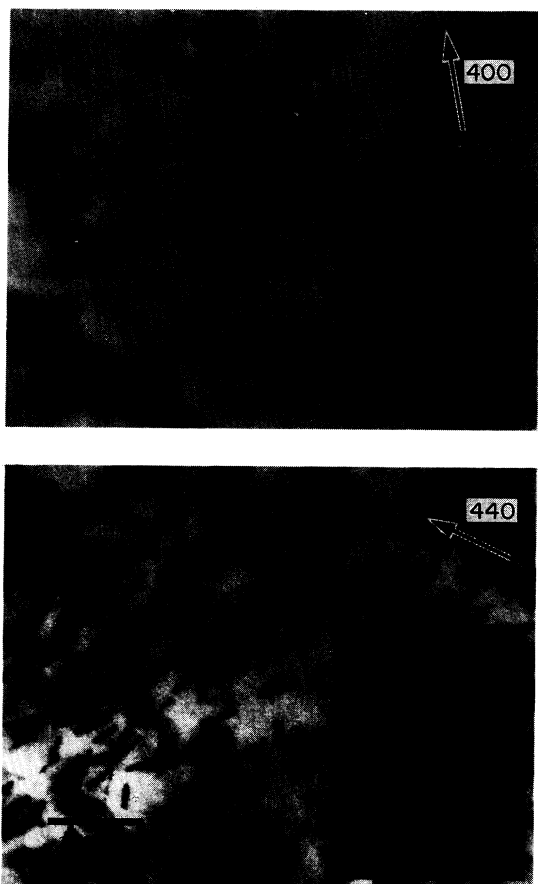


FIG. 1. Bright field TEM images of columnar defect tracks viewed nearly end on for 1.08-GeV Au (top) and 0.58-GeV Sn (bottom) irradiations of single crystals of YBCO. The irradiated crystals were thinned to a depth of $23\ \mu\text{m}$ in the Au case and to a depth of $19\ \mu\text{m}$ in the Sn case. The crystals have been tilted in the electron microscope such that the tracks are inclined by approximately 10° relative to the electron beam direction. In recording these images, weak diffracting conditions were established using 400 (top) and 440 (bottom) scattering reflections to minimize strain effects surrounding the defects. The resulting perspective views of the defects exhibit significant directional misalignment from the approximate median direction indicated by the double ended arrows. The radial angular distribution of the track directions around the median has been measured from similar images at different depths and is shown in Fig. 2 along with computed values. Insets show the respective cross sections for the two irradiations at $21\ \mu\text{m}$ depth for Au and $8\ \mu\text{m}$ for Sn. The splay in the track directions is visible in both.

Hwa and co-workers⁵ suggested that a splay in the orientation of the columns will lead to an “entangled” state of the vortex matter, a “splayed glass,” in which the “phase space” for the hopping and spreading processes is substantially reduced; it may be of energetic advantage for a vortex segment to hop to the nearest defect, but it may be prohibitive by the geometry—the price to be paid is the increase in the elastic energy. The implied consequence of such disorder is a larger critical current density J_c than for the parallel (unsplayed) columns of damage and a greatly diminished flux creep.⁵

To test the suggestion of Hwa *et al.*, we inspect the damage produced in single crystals of YBCO by the irradiation with 0.58-GeV $^{116}\text{Sn}^{30+}$ and 1.08-GeV $^{197}\text{Au}^{23+}$.⁹ The incident ions transfer their energy primarily to the electronic system, with rates exceeding $2\ \text{keV}/\text{\AA}$ for Sn and $4\ \text{keV}/\text{\AA}$ for Au. The damage consists of nearly aligned columns of amorphized material, $50\text{--}70\ \text{\AA}$ in diameter, randomly distributed in the plane normal to the beam.¹⁰ The cross sectional transmission electron microscopy (TEM) images for both irradiations shown in the insets of Fig. 1 confirm that while the tracks are predominantly parallel, there are a few wayward tracks which stray. The splay in the paths of damage is due to Rutherford scattering caused by the rare events of almost frontal collisions with a nucleus in the target, and should be more pronounced for the less massive Sn ions. This expectation is confirmed by the bright field nearly end-on TEM images at a $23\ \mu\text{m}$ depth for Au (Fig. 1, top) and a $19\ \mu\text{m}$ depth for Sn (Fig. 1, bottom) which clearly show that at comparable depths, the Sn irradiation is more splayed. The analysis of the angular distributions of tracks, such as those shown in Fig. 1, was carried out on the images at different depths and compared with the TRIM Monte Carlo calculations.¹¹ The result is shown in Fig. 2, where the splay is defined as the median angular dispersion of the tracks, relative to the incident beam

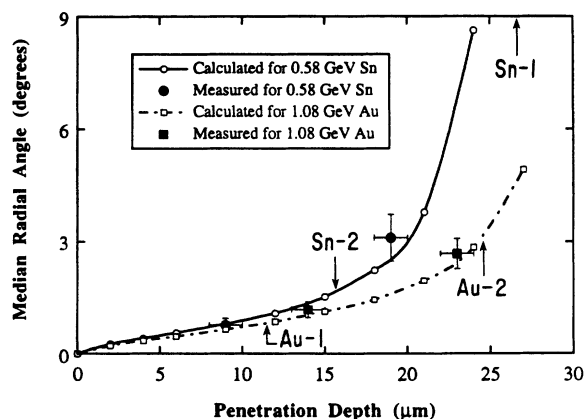


FIG. 2. The median angular divergence of columnar tracks, relative to the irradiation direction, vs depth in YBCO crystals, produced by 0.58-GeV Sn and 1.08-GeV Au. The Monte Carlo calculation is shown by the connected open symbols. The solid symbols are the values obtained from TEM micrographs, such as shown in Fig. 1. Arrows indicate the thicknesses of the magnetically examined crystals; Au-1 and Sn-1 with a large difference in splay (see Figs. 3 and 4) and Au-2 with Sn-2 with similar splay (inset of Fig. 4).

direction. Note that the Monte Carlo calculation agrees remarkably well with the amount of splay deduced from TEM images. This figure unambiguously demonstrates that the *growth of the splay as the ions penetrate the crystal is much larger for Sn than for Au*. The splay difference becomes dramatic as we approach the projected ranges of both ions in YBCO, which are about $27\ \mu\text{m}$ for Sn and $32\ \mu\text{m}$ for Au.¹⁰

Thus, if we compare a $11.5\text{-}\mu\text{m}$ thick crystal irradiated with Au and a $27\text{-}\mu\text{m}$ thick crystal irradiated with Sn, the splay difference will be about 10° , quite large, and, if Hwa's suggestion is correct, at a comparable dose we should see large differences in persistent currents J . Figures 3 and 4 show the variation of the persistent currents with temperature for such two YBCO single crystals irradiated at nearly the same doses; $B_\phi = 4.7\ \text{T}$ for Au and $B_\phi = 5\ \text{T}$ for Sn. The matching field B_ϕ is a convenient way to express the density of columnar defects; it is the field at which the density of vortices and defects are equal.¹² The current density J was obtained from the measurements of irreversible magnetization $M(H, T)$ via the critical state model,¹³ which relates J and M through a geometrical (shape) factor. $M(H, T)$ and its time decay was measured in a commercial SQUID (superconducting quantum interference device) magnetometer with the magnetic field applied 2° off the c axis, the direction of the incident beam.¹⁴ Figure 3(a) shows J normalized to $J(5\ \text{K})$ vs T for $H = 1\ \text{T}$. The $J(5\ \text{K})$ of the two crystals are nearly identical; $J^{\text{Sn}}(5\ \text{K}) \sim 1.1J^{\text{Au}}(5\ \text{K})$ with about 20% uncertainty due to the geometrical factor. The tem-

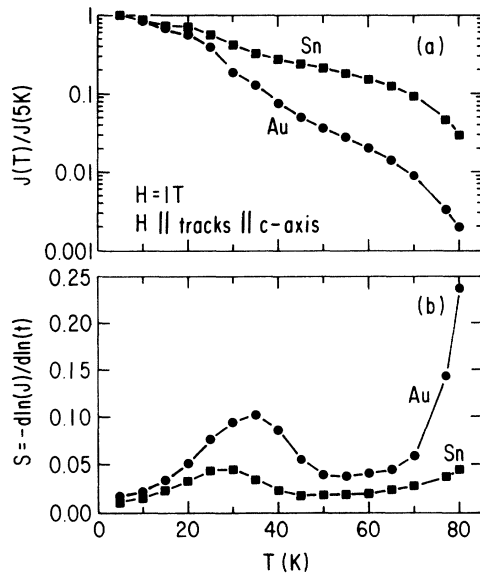


FIG. 3. (a) The persistent current density J normalized to its value at 5 K, plotted vs temperature, in a 1 T magnetic field aligned with the mean track direction. At $T = 5\ \text{K}$, $J = 9.45 \times 10^6\ \text{A/cm}^2$ for the crystal irradiated with Sn ions (solid squares) to a dose equivalent to a matching field $B_\phi = 5.0\ \text{T}$. $J = 8.4 \times 10^6\ \text{A/cm}^2$ for the crystal irradiated with Au (dots) to a dose 4.7 T. (b) The normalized logarithmic flux creep rate S for the same two crystals. The current density is higher for the more splayed Sn-irradiated crystal and the creep rate is lower.

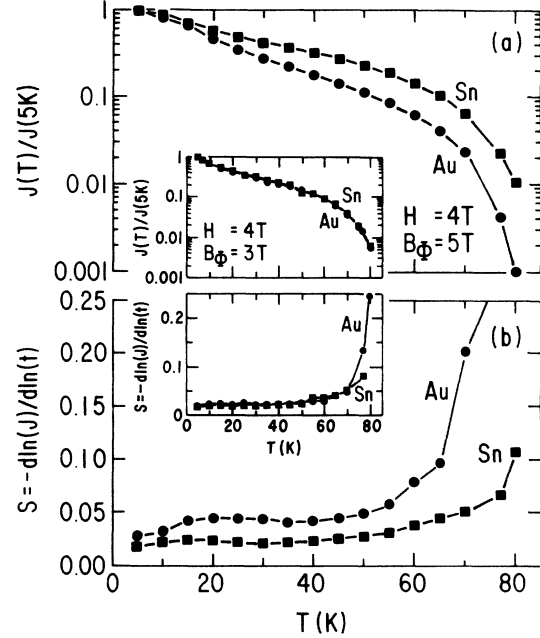


FIG. 4. (a) The normalized current density and (b) creep rate, as in Fig. 3, measured in a 4-T field, where the densities of vortices and columnar defects are comparable. At $T = 5\ \text{K}$, $J = 5.34 \times 10^6\ \text{A/cm}^2$ for the Sn-irradiated crystal (solid squares) and $J = 3.2 \times 10^6\ \text{A/cm}^2$ for the crystal irradiated with Au (dots). The inset shows $j(T)/J(5\ \text{K})$ (top) and $S(T)$ (bottom) for the two crystals irradiated with Sn [$B_\phi = 3\ \text{T}$, $J(5\ \text{K}) = 4.3 \times 10^6\ \text{A/cm}^2$] and with Au [$B_\phi = 2.4\ \text{T}$, $J(5\ \text{K}) = 2.57 \times 10^6\ \text{A/cm}^2$] that have similar splay. The temperature dependences are identical.

perature dependences, however, are remarkably different; $J^{\text{Au}}(T)$ decreases more rapidly with increasing temperature than $J^{\text{Sn}}(T)$. Indeed, in the temperature range between 70–80 K, the difference in J between the two irradiations is, quite remarkably, about an *order of magnitude*. Since the critical current densities $J_c \approx J(5\ \text{K})$ are similar, the larger high-temperature $J(T)$ in the Sn-irradiated YBaCuO crystal should be linked to a slower relaxation of vortices there. And, if this is so, we argue that the relaxation, or creep, is reduced to a considerable degree by a splay of $\sim 10^\circ$ in the orientation of the columns of damage. We confirm this by the data in Fig. 3(b), showing the normalized relaxation rates $S = d \ln(J)/d \ln(t)$ for the above two crystals for the same field as a function of temperature. S was measured by sweeping H to a $-5.5\ \text{T}$ (to ensure complete field penetration), increasing it to the target field (here $+1\ \text{T}$), and recording $M(t) \propto J(t)$ for approximation 2 hours (during this short time window the time dependence of S due to the nonlogarithmicity of the decay is undetectable). At low temperatures the relaxation rates are similar. Since at low temperatures $S \sim kT/U$, where U is the activation energy for vortex jumps, we estimate from the initial slope the effective single track pinning energy⁷ $U_p \approx 400\text{--}600\ \text{K}$ for both. This is not surprising, since the reduction of U_p by the loss of elastic energy due to a small splay⁵ is small. As the temperature is increased, so is S , which reaches a *flat* maximum around 30–40 K.

Here, the ratio $S^{\text{Au}}/S^{\text{Sn}} \sim 2$. This ratio is maintained until ~ 65 K, although S for both crystals has declined by a factor of about 2 as well. Above 65 K, S increases dramatically for Au, but less for Sn the ratio at 80 K is 5, entirely consistent with large differences in J .

The *nonmonotonic temperature dependence* of S , i.e., a flat maximum around 40 K, is clearly due to the columnar tracks; we have never observed this effect either in virgin or in the proton-irradiated crystals.¹⁵ It possibly reflects crossing of different collective pinning regimes⁸ as we traverse the H - T phase diagram from 5 K up to T_c . At low fields the pinning is expected to be strong (single-vortex pinning) over a significant range of temperatures,⁸ and becomes weak (collective) due to vortex-vortex interactions only in the vicinity of T_c . At high fields, the pinning will be always collective.⁸ Thus, we expect $S(T)$ to reflect the crossover at low fields (below $\sim 0.5B_\phi$),¹⁶ but not at high fields. The data of Fig. 4 confirm this. Figure 4(b) shows normalized S 's of our crystals at $H = 4$ T. Indeed, $S(T)$ is monotonic in temperature; the maximum has disappeared. The ratio of $S^{\text{Au}}(T)/S^{\text{Sn}}(T)$ at 80 K is ~ 3.5 , slightly smaller than for $H = 1$ T, consistent with the differences in U [see Fig. 4(a)].

In addition to the differences in splay, the defects produced by Sn and Au irradiations differ slightly in diameter and continuity.¹⁰ To be sure that the observed differences in $J(T)$ and S are due to splay, and not to other factors, we have also studied two other YBCO crystals irradiated with Sn and Au, whose thicknesses were selected to produce a similar splay. We compared a $15.6\text{-}\mu\text{m}$ thick crystal irradiated with Sn and a $24.7\text{-}\mu\text{m}$ thick crystal irradiated with Au, to doses $B_\phi = 3$ T and $B_\phi = 2.4$ T, respectively. From Fig. 2, we estimate splays to be comparable; $\sim 1.8^\circ$ and $\sim 3^\circ$, respectively. We expect then the differences in J and S to be small and this is indeed seen in the insets of Fig. 4; the temperature dependences of J are nearly identical for the two crystals, with the

creep rates corresponding closely as well.

Thus, our results show that the splay in the orientation of the columnar defects has a significant effect on the dynamics of vortices. We note that large differences in splay angles occur only near the end of the ion ranges; i.e., in a small fraction of the sample thickness. Close to the top surface, splay angles for Sn and Au are small and nearly identical. Hence, there is an induced inhomogeneity along the crystal thickness, which makes it difficult to quantify the effect, and it is obvious that the resulting pinning enhancement is not optimized here. Nevertheless, it can inhibit the motion of vortices and enhance persistent currents at least by an order of magnitude. Clearly, with the optimization of splay⁵ this may lead to significant advances in technology. Although the theory of Hwa *et al.*⁵ considers only the low field regime, we show that the splay plays a significant role at high fields as well. The actual divergence of the effective pinning barriers at low currents remains to be determined from the decay of the persistent currents over very long periods of time.

This work was partly sponsored by the Division of Material Sciences, U.S. Department of Energy, Office of Advanced Utilities Concepts-Superconductivity Partnership Program under Contract No. DE-AC-05-84OR21400 with Martin Marietta Energy Systems, Inc. Part of the work of J.R.T. and Y.R.S. was supported by the Science Alliance at the University of Tennessee. The work of M.A.K. and R.W. was supported by the U.S. Department of Energy, BES-Materials Sciences, under Contract No. W-31-109-Eng-38, and NSF (DMR 91-20000) through the Science and Technology Center for Superconductivity. We thank J. Hardy and J. Forster at TASCC (Chalk River) for their help and the provision of irradiation facilities. The operation of TASCC is supported by AECL Research.

*Present address: Centro Atomico Bariloche, 8400 Bariloche, Argentina.

¹L. Civale, A. D. Marwick, T. K. Worthington, M. A. Kirk, J. R. Thompson, L. Krusin-Elbaum, Y. Sun, J. R. Clem, and F. Holtzberg, *Phys. Rev. Lett.* **67**, 648 (1991).

²M. Konczykowski, F. Rullier-Alebeque, E. R. Jacoby, A. Shaulov, Y. Yeshurun, and P. Lejay, *Phys. Rev. B* **44**, 7167 (1991).

³R. C. Budhani, M. Suenaga, and S. H. Liou, *Phys. Rev. Lett.* **69**, 3816 (1992).

⁴J. R. Thompson, Y. R. Sun, H. R. Kerchner, D. K. Christen, B. C. Sales, B. C. Chakoumakos, A. D. Marwick, L. Civale, and J. O. Thomson, *Appl. Phys. Lett.* **60**, 2306 (1992).

⁵T. Hwa, P. LeDoussal, D. R. Nelson, and V. M. Vinokur, *Phys. Rev. Lett.* **71**, 3545 (1993).

⁶A. I. Larkin and Yu. N. Ovchinnikov, *Zh. Eksp. Teor. Fiz.* **65**, 1704 (1973) [*Sov. Phys. JETP* **38**, 854 (1974)]; *J. Low Temp. Phys.* **34**, 409 (1979).

⁷M. V. Feigel'man, V. B. Geshkenbein, A. I. Larkin, and V. M. Vinokur, *Phys. Rev. Lett.* **63**, 2301 (1989); A. P. Malozemoff and M. P. A. Fisher, *Phys. Rev. B* **42**, 6784 (1990).

⁸D. R. Nelson and V. M. Vinokur, *Phys. Rev. Lett.* **68**, 2398 (1992); *Phys. Rev. B* **48**, 13 060 (1993).

⁹The crystals were irradiated with Sn at the Holifield Facility at

Oak Ridge National Laboratory, and with Au at the Tandem Accelerator Superconducting Cyclotron (TASCC) facility at the Chalk River Laboratories in Canada.

¹⁰A. D. Marwick, L. Civale, L. Krusin-Elbaum, R. Wheeler, J. R. Thompson, T. K. Worthington, M. A. Kirk, Y. R. Sun, H. R. Kerchner, and F. Holtzberg, *Nucl. Instrum. Methods B* **80/81**, 1143 (1993); R. Wheeler *et al.* (unpublished).

¹¹J. F. Ziegler, J. B. Biersack, and U. Littlemark, *The Stopping Range of Ions in Solids* (Pergamon, New York, 1985), p. 79.

¹²For example, $B_\phi = 5$ T corresponds to a dose 2.4×10^{11} ions/cm² and $B_\phi = 4.7$ T corresponds to 2.28×10^{11} ions/cm².

¹³C. P. Bean, *Rev. Mod. Phys.* **36**, 31 (1964).

¹⁴All irradiations were done with the incident beam 2° off the c axis to avoid axial channeling.

¹⁵J. R. Thompson, Y. R. Sun, D. K. Christen, H. R. Kerchner, A. P. Malozemoff, L. Civale, A. D. Marwick, T. K. Worthington, L. Krusin-Elbaum, M. W. McElfresh, and F. Holtzberg, in *Physics and Materials Science of High Temperature Superconductors-II*, Vol. 209 of *NATO Advanced Study Institute, Series E: Applied Sciences*, edited by R. Kossowsky (Plenum, New York, 1992), pp. 573–93.

¹⁶L. Krusin-Elbaum, L. Civale, G. Blatter, A. D. Marwick, F. Holtzberg, and C. Feild, *Phys. Rev. Lett.* **72**, 1914 (1994).

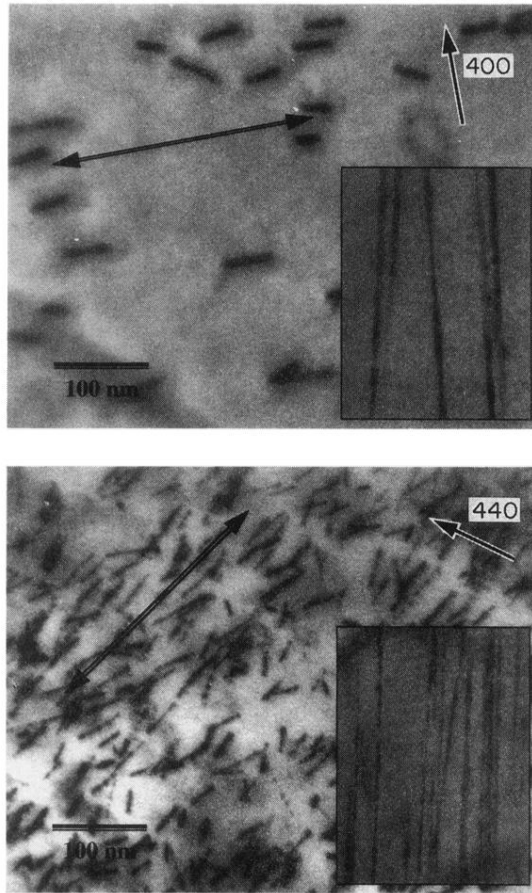


FIG. 1. Bright field TEM images of columnar defect tracks viewed nearly end on for 1.08-GeV Au (top) and 0.58-GeV Sn (bottom) irradiations of single crystals of YBCO. The irradiated crystals were thinned to a depth of $23\ \mu\text{m}$ in the Au case and to a depth of $19\ \mu\text{m}$ in the Sn case. The crystals have been tilted in the electron microscope such that the tracks are inclined by approximately 10° relative to the electron beam direction. In recording these images, weak diffracting conditions were established using 400 (top) and 440 (bottom) scattering reflections to minimize strain effects surrounding the defects. The resulting perspective views of the defects exhibit significant directional misalignment from the approximate median direction indicated by the double ended arrows. The radial angular distribution of the track directions around the median has been measured from similar images at different depths and is shown in Fig. 2 along with computed values. Insets show the respective cross sections for the two irradiations at $21\ \mu\text{m}$ depth for Au and $8\ \mu\text{m}$ for Sn. The splay in the track directions is visible in both.